PHYSICAL REVIEW D **84,** 105036 (2011)

High speed collision and reconnection of Abelian Higgs strings in the deep type-II regime

G. J. Verbiest*
Instituut-Lorentz for Theoretical Physics, Leiden, The Netherlands

A. Achúcarro†
Instituut-Lorentz for Theoretical Physics, Leiden, The Netherlands, and Departamento de Física Teórica, Universidad del País Vasco UPV-EHU, Bilbao, Spain

(Received 16 June 2011; published 22 November 2011)

We study the high speed collision and reconnection of Abrikosov–Nielsen–Olesen cosmic strings in the type-II regime of the Abelian Higgs model, that is, scalar-to-gauge mass ratios larger than 1. Qualitatively, new phenomena such as multiple reconnections and clustering of small-scale structure have been observed in the deep type-II regime and reported in a previous paper, as well as the fact that the previously observed ''loop'' that mediates the second intercommutation is only a loop for sufficiently large mass ratios. Here we give a more detailed account of our study, which involves 3D numerical simulations with the parameter $\beta = m^2_{\text{scalar}}/m^2_{\text{gauge}}$ in the range $1 \leq \beta \leq 64$, the largest value simulated to date, as well as 2D simulations of vortex-antivortex head-on collisions to understand their possible relation to the new 3D phenomena. Our simulations give further support to the ideas that Abelian Higgs strings never pass through each other, even at ultrarelativistic speeds, unless this is the result of a double reconnection; and that the critical velocity for double reconnection goes down with increasing mass ratio, but energy conservation suggests a lower bound around 0.77 c. We discuss the qualitative change in the intermediate state observed for large mass ratios. We relate it to a similar change in the outcome of 2D vortex-antivortex collisions in the form of radiating bound states, whereas we find no evidence of the back-to-back reemergence reported in previous studies. In the deep type-II regime the angular dependence of the critical speed for double reconnection does not seem to conform to the semianalytic predictions based on the Nambu-Goto approximation. We can model the high angle collisions reasonably well by incorporating the effect of core interactions, and the torque they produce on the approaching strings, into the Nambu-Goto description of the collision. An interesting, counterintuitive aspect is that the effective collision angle is smaller (not larger) as a result of the torque. Our results suggest differences in network evolution and radiation output with respect to the predictions based on Nambu-Goto or $\beta = 1$ Abelian Higgs dynamics.

DOI: 10.1103/PhysRevD.84.105036 PACS numbers: 11.27.+d, 98.80.Cq

I. INTRODUCTION

The discovery of cosmic strings would revolutionize our understanding of particle physics at the extremely high energies present in the very early Universe. Cosmic strings, first proposed by Kibble [1], could signal a ''superconducting'' phase transition and give information on the particle interactions before the transition, or they might provide the first evidence of superstring theory. So far there is no evidence of their existence, but strings can lead to a wealth of detectable astrophysical phenomena and there is an increasing number of surveys and searches looking for observable signatures. These include cosmic microwave background anisotropies, gravitational lensing, wakes, gravitational radiation, cosmic rays and gamma ray bursts, among others. Gravitational effects are determined by the adimensional parameter $G\mu$ which for most models of cosmological interest falls in the range 10^{-13}–10^{-6}. (We use units with $\hbar = c = 1$ throughout; G is Newton's constant and μ the mass per unit length of the strings.) Strings with higher mass per unit length are already ruled out by these observations (see the classic reviews [2–5] and the more recent updates [6–11], and references therein).

The formation of cosmic strings and superstrings is a generic outcome of cosmological phase transitions [1] and of some inflationary models, in particular, those based on grand unified theories [12,13]. More recently, it has been appreciated that some models of brane inflation could also lead to cosmic superstrings [14,15]. Once formed, a string network is expected to reach a scaling solution in which statistical properties such as the distance between strings or the persistence length become a fixed fraction of the horizon size (the age of the Universe). The energy density in strings decreases with time, but the expansion of the Universe pumps energy into the string network—by increasing the contribution of long strings—and this is balanced by energy losses to radiation. If these are efficient enough, the contribution from the strings to the energy density of the Universe remains a small, constant fraction

*Verbiest@physics.leidenuniv.nl
†Achucar@lorentz.leidenuniv.nl

of the dominant form of energy (matter or radiation) and is potentially observable. Radiation is emitted by oscillating loops, formed when a string self-intersects, and in bursts. The latter are produced by cusps (sections of the string which acquire near-luminal speeds), by the final stages of collapsing loops and, to a lesser extent, by kinks created when strings reconnect. The reconnection, or *intercommutation* of strings is therefore an essential process that determines and maintains the long-term scaling behavior of the string network.

In this paper, which is a companion to [16], we focus on the high speed intercommutation of Abelian Higgs strings in the deep type-II regime. The terminology is borrowed from superconductors, where type-I (type-II) indicates a critical parameter $\beta < 1$ ($\beta > 1$); β is the ratio of scalar-to-gauge excitation masses, squared (see below). An important difference between type-I and type-II is the interaction energy between parallel vortices, which is attractive for type-I and repulsive for type-II [17]. Cosmic string intercommutation was first investigated numerically by Shellard for global strings [18] and later by Matzner for type-II $\beta = 2$ Abelian Higgs strings [19]. They pointed out that in ultrarelativistic collisions there is a critical center-of-mass velocity v_c (depending on the collision angle) beyond which strings pass through: a loop forms, expanding rapidly from the collision point, that catches up with the reconnected strings and produces a second intercommutation. A more recent study [20] focused on double reconnection and showed that it proceeds differently in type-I and type-II strings, with the loop forming only in type-II collisions. In fact, one of the main results in [16] that we elaborate on here is that the loop forms only in deep type-II ($\beta \gg 1$) collisions. Although we do not determine the precise value of β for which the transition occurs, it is somewhere between $\beta = 8$ and $\beta = 16$. For $\beta \geq 16$, we see the loop forming, while type-II collisions with $\beta \leq 8$ produce instead a ''blob'' of radiation that can look like a loop but is not (see later sections and [16]). Another important point is the angular dependence of v_c as a function of the collision angle. In Ref. [20], it was shown that it is dictated by the geometry and speeds of the strings after the first reconnection, which can be calculated in the Nambu-Goto approximation. In the deep type-II regime, we expect core interactions to play an increasingly important role, even before the collision, and this is indeed what we will report here.

The simulations in [20] had decreasing resolution with increasing β, and explored only two values of β in the type-II regime ($\beta = 8, 32$), but the results suggested that the critical velocity for the second reconnection would go down as a function of β. This is interesting because one of the distinguishing features of cosmic superstrings, as opposed to the Abrikosov–Nielsen–Olesen (ANO) strings [21,22] considered here, is their low intercommutation probability $P \sim 10^{-3}$–10^{-1} [23], which leads to different scaling properties, in particular, to denser networks (although in an expanding background the effect is weaker than the $\rho t^2 \sim 1/P$ dependence one might expect for the density ρ at cosmic time t [24]). However, if the critical velocity of strongly type-II Abelian Higgs strings decreases to the extent that it becomes comparable to the average velocity of the network, the *effective* intercommutation probability could be much less than 1. This was one of the motivations behind the present study.

Our results confirm the claim of [20] that the critical velocity for the second reconnection goes down as a function of β, although energy conservation suggests this decrease cannot go on indefinitely. We will return to this point later. Furthermore, while studying the critical velocity, we found multiple intercommutations. That is, processes where the strings exchange ends 3 times or more. We found multiple reconnections only for $\beta \geq 16$. We will show that this is related to a qualitative change in the nature of the intermediate state, from localized radiation to a string loop, which determines the process leading to the second intercommutation. For $1 < \beta \leq 8$, we found that the previously reported loop is just an expanding blob of radiation, while for $\beta \geq 16$ we find a topological loop rapidly expanding from the collision point.

An interesting question that was not addressed in [16] is whether these multiple reconnections and the blob-to-loop transition could be related to, for instance, two-dimensional bound states of the vortex-antivortex system or whether they are a purely three-dimensional effect. In order to shed light on this connection, we also simulated the high speed head-on collision of a vortex and an antivortex in 2D. Abelian Higgs vortex-antivortex scattering in two dimensions was studied years ago by Myers, Rebbi and Strilka [25] (see also [26]). They reported that, beyond a certain critical speed, the vortices reemerge, and the way in which they reemerge depends on β: for $\beta \leq 4$, they bounce back, and for $\beta \geq 8$, they pass through (and for velocities below the critical speed the pair annihilates into radiation). For large β, we agree with their results: we found that, for $\beta \geq 6.4$, the vortices reemerge as if they have passed through. However, for $\beta \leq 6.2$, we find no evidence of backscatter; instead, we always find a bound radiating state. The energy profile looks as if the vortex-antivortex have passed through, but a closer look at the magnetic field shows they are just fluctuations. They cannot escape each other's influence, and radiation keeps being emitted from the area around the collision point until all the energy has been radiated away. As we will discuss, these two behaviors are consistent with the change we observe in the intermediate state in 3D collisions. The ''pass through'' behavior at high β corresponds to a 3D loop, while the 2D radiating bound states at low β correspond to the 3D blob. On the other hand, the relation with multiple reconnections is more subtle, and it appears that the number of reconnections is mainly a three-dimensional effect.

II. A FEW COMMENTS ON COSMIC STRING INTERCOMMUTATION

String intercommutation poses some interesting puzzles from a theoretical point of view. ANO strings are topological; they cannot break. When two string segments collide, there are, in principle, three possible outcomes:

(a) They can exchange partners and reconnect (intercommute). The reconnected strings have a slightly shorter length. This is the default outcome and, as we shall discuss, seems to occur *always* when Abelian Higgs strings meet.

(b) In near-parallel collisions of type-I strings at low velocity, the attractive interaction makes them stick together, e.g. type-I Abelian Higgs strings [27,28]. The network then has junctions between strings with different winding numbers (and different energy per unit length). String networks with junctions have been extensively studied analytically in the Nambu-Goto approximation [29,30], and in this regime they give an extremely good fit to numerical simulations [31].

(c) The strings can simply pass through each other. The relative probability of outcomes (a) and (c) is an important distinguishing feature of ANO strings versus cosmic (super)strings. The intercommutation of fundamental superstrings, and of D-strings, is a quantum process and, as such, has some probability of not happening [32]. This is also an expected feature of higher-dimensional models—in which the apparent collision of the strings can be a four-dimensional illusion; the strings are actually not intersecting in the higher-dimensional space—or models with extra internal degrees of freedom [4,33]. Cosmic superstrings have been shown to give reconnection probabilities (P) as low as $P \sim 10^{-3}$–10^{-1} [23].

An interesting observation is that one would naïvely expect outcome (c) to be the result of any sufficiently fast collision of ANO strings, since the natural time scales of the microscopic fields can be much slower than the string crossing time [34]. In the case of domain walls, for instance, the scalar field profiles pass through each other undistorted in ultrarelativistic collisions [35]. The head-on collision of a vortex and an antivortex in 2D at ultrarelativistic speeds is also known to result in the two passing through each other [25]. However, this "free passage" is not observed in 3D string collisions. In the Abelian Higgs model, all (numerical) evidence to date [16,19,20] points to the conclusion that $P = 1$: ANO strings with unit winding *always reconnect at least once, even at ultrarelativistic speeds*. (Even in case (b), there is some evidence that the strings will first reconnect and then settle into a junction [31]). What is observed, instead, is that, beyond a certain critical collision velocity v_c, the strings may reconnect a second time and effectively pass through with some distortion. In terms of network evolution, this is as if the strings have not reconnected, and one can talk of an *effective* intercommutation probability $P_{\rm eff}$ being less than 1. An important question is to model the dependence of the critical velocity for nonreconnection as a function of collision speed and angle, and to understand its dependence with β.

At lower speeds, an interesting class of analytic results on intercommutation is based on the moduli space approximation [36]. In the Bogomol'nyi limit ($\beta = 1$) [37], the moduli space or geodesic approximation gives a very good description of slow vortex-vortex collisions in two dimensions and predicts the observed right-angle scattering[38]. Although these arguments are valid only at low speeds and in the absence of core interactions, they lead to the expectation that, in three-dimensional collisions, reconnection is inevitable. Consider the configuration in Fig. 1(a), two strings colliding with angle α and velocity v. If the incoming strings lie in the yz plane and move in the x-direction, the collision looks in the xz plane like two vortices that will scatter at 90° [26,38,39], while in the xy plane it is a vortex-antivortex collision, which we expect will annihilate. In 3D the energy from this annihilation goes into creating the connecting segments, and the rest is emitted as radiation.

This idea has been extended to other models such as D-strings [40] and non-Abelian strings [33,41]. In many cases, intercommutation is expected with probability 1 in the regime of validity of the moduli space approximation, which—as we just emphasized—requires two conditions: low speed, so that higher order frequency modes are not excited, and negligible core interactions (such as in near-parallel collisions not far from the Bogomol'nyi limit).

It is worth stressing that, even if these conditions are satisfied before the collision, they will not hold after intercommutation because the "new" portions of string that are generated between the receding strings are necessarily

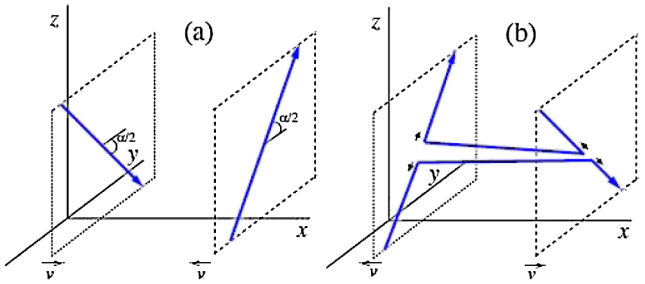

FIG. 1 (color online). From Ref. [20] (a) Initial positions and orientations of the strings in the center-of-mass frame. The strings lie in the $x = \text{const}$ planes and approach each other with speed v. The arrows indicate the orientations of the strings, which form an angle α. (b) The configurations after one intercommutation. If $v \sim c$, the kinks' motion along the strings is negligible and the connecting horizontal segments are practically antiparallel and immobile, making a second interaction possible.

almost antiparallel around the point of collision, and their core interactions are crucial in understanding what happens next. This is probably the reason why a prediction for the angular dependence of the critical speed in [40] fails to agree with the data from numerical simulation. This prediction is based on an energy argument which does not take into account the interaction between the string cores, and this approximation fails immediately *after* the collision.

By using the thin string approximation and taking into account the effect of core interactions after the collision, Ref. [20] obtained a semianalytic expression for the critical velocity for double reconnection v_c as a function of the collision velocity v and angle α. This works quite well for type-I and moderately type-II ANO strings. Consider the situation in Fig. 1(b) after the first intercommutation. Within the Nambu-Goto approximation—thus ignoring core interactions– we can express the angle δ between the horizontal segments and the speed w at which the horizontal segments move apart in terms of v and α:

$$w = \sin(\alpha/2)/\gamma(v), \tag{1}$$

$$\cos(\delta/2) = \frac{\cos(\alpha/2)/(v\gamma(v))}{\sqrt{1 + (\cos(\alpha/2)/(v\gamma(v)))^2}}. \tag{2}$$

Notice that for high collision speeds the horizontal segments are almost antiparallel, $\delta \sim \pi$, and they move slowly, $w \sim 0$. If they are not receding very fast, the antialigned segments will be attracted to each other and will annihilate, causing the strings to reconnect a second time. In the unphysical limit of a collision at the speed of light, the bridging segments would not move at all and would be antiparallel, so the second reconnection is expected with probability 1. The angular dependence of the threshold speed v_c is then found with Eqs. (1) and (2) if one assumes that reconnection will happen below a threshold "escape" speed w_t and above a threshold angle δ_t, close to antiparallel. The threshold values w_t and δ_t are left as free parameters and determined by the best fit to the numerical data. While this model works well near the Bogomol'nyi limit $\beta \sim 1$, we will show that it does not work so well in the deep type-II regime studied here, indicating that core interactions before the collision are also important. We will return to this point in the discussion.

Equation (1) shows that fast collisions will produce very slowly moving connecting segments. Conversely, a slow collision usually creates a highly curved region after intercommutation, which will accelerate under its own tension and acquire large speeds. This is one of the mechanisms that helps the string network maintain a typical speed $\langle v^2 \rangle \sim 0.5$, even in an expanding Universe.

III. SIMULATIONS

The Abelian Higgs model is the relativistic version of the Ginzburg-Landau model of superconductivity. It is described by the Lagrangian

$$\mathcal{L} = (\partial_\mu + ieA_\mu)\phi(\partial^\mu - ieA^\mu)\phi^\dagger - \frac{1}{4}F^{\mu\nu}F_{\mu\nu} - \frac{\lambda}{4}(|\phi|^2 - \eta^2)^2, \tag{3}$$

where ϕ is a complex scalar field and A_μ is a U(1) gauge field with field strength $F_{\mu\nu} = \partial_\mu A_\nu - \partial_\nu A_\mu$ ($\mu, \nu = 0, 1, 2, 3$).

The ground state has $|\phi| = \eta$ and zero electric and magnetic field. The fluctuations about this vacuum define two mass scales: the scalar excitations have $m_{\text{scalar}} = \sqrt{\lambda}\eta$ and the gauge field excitations, $m_{\text{gauge}} = \sqrt{2}e\eta$. Classically, the only relevant parameter in the dynamics is their ratio, $\beta = (m_{\text{scalar}}/m_{\text{gauge}})^2 = \lambda/2e^2$, which also characterizes the internal structure of the ANO vortices.

Magnetic cores repel and scalar cores attract, so the interaction between vortices is determined by which of these cores is the larger: parallel ANO vortices repel for $\beta > 1$ and attract for $\beta < 1$. The Bogomol'nyi limit $\beta = 1$ is a critical value where both effects cancel and parallel vortices do not interact. In this paper we are interested in the $\beta > 1$ regime, analogous to a type-II superconductor, and in this case the vortices have an inner "scalar" core of radius $\sim m_{\text{scalar}}^{-1}$ in which the scalar field departs from its vacuum value and vanishes at the center. This is surrounded by a larger, "gauge" core of radius $\sim m_{\text{gauge}}^{-1}$ where the magnetic field is nonzero. The repulsive interaction produces a torque that tends to antialign two colliding strings. This will play an important role later.

Here, as in [16], we follow the numerical strategy of [19,20]: we use a lattice discretization and place a superposition of two oppositely moving ANO strings on a three-dimensional lattice. This configuration is evolved using a leapfrog algorithm. The initial configuration is determined by two parameters: the center-of-mass speed v of the strings when they are far apart and the angle α between them. (Every collision can be brought to this form by an appropriate Lorentz transformation [18].)

We also impose "freely moving" boundary conditions: after each round, the fields inside the box are updated using the equations of motion, and the fields on the boundaries are calculated assuming the strings move unperturbed and at constant speeds at the boundaries.

All 3D simulations were done on a $200 \times 200 \times 400$ grid. Unless otherwise stated, we use a lattice spacing $a = 0.2$ and time steps $\Delta t = 0.02$, so the Courant condition (here, $\Delta t \leq a/\sqrt{3}$) holds. Some simulations were repeated with $a = 0.1$, in particular, those with $\beta = 4$, to confirm the results.

Our simulations are optimized for the deep type-II regime. By solving the two-dimensional, static vortex equations, one finds that in a static straight cosmic string about half of the potential energy in the scalar core is contained within a radius $\sqrt{2}m_{\text{scalar}}^{-1}f(\beta)$, where f is a slowly varying function with $f(1) = 1$, $f(64) = 1.4$. Lorentz contraction gives an extra factor $\gamma(v)^{-1}$ in the direction of approach,

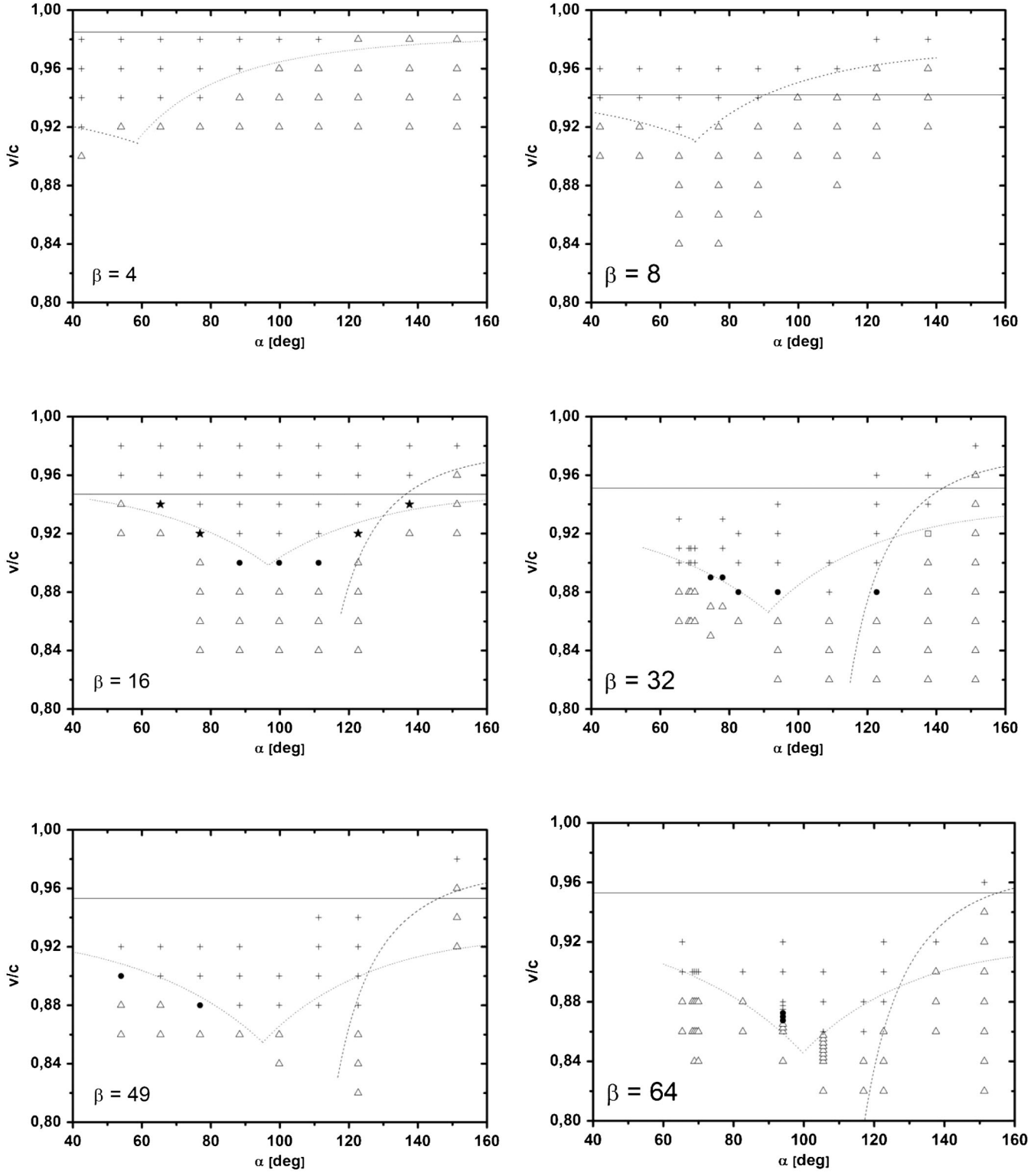

FIG. 2. The number of intercommutations for a range of collision velocities and angles for $\beta = 4$, 8, 16, 32, 49 and 64. The symbols $\triangle$, $+$, $\bullet$ and $\star$ stand for 1, 2, 3 or 4 intercommutations, respectively. The dotted lines show a two-parameter fit to simulations with collision angles below 150°, based on the Nambu-Goto approximation [20] The dashed line is a one-parameter fit adapted to the deep type-II regime at high collision angle. (See text for explanation and fit parameters.) Simulations above the horizontal line resolve the scalar core size by less than three lattice points and are therefore less reliable. The point at ($\beta = 32$, $\alpha = 137.6$, $v = 0.92$), indicated by a square $\square$, is inconclusive because the intercommutation happens just beyond the dynamical range. The $\beta = 4$ simulation has lattice spacing $a = 0.1$; all others have $a = 0.2$.

with $\gamma(v) = 1/\sqrt{1 - v^2}$. This is the smallest length scale that has to be resolved. Without loss of generality we take $\lambda = 2$, $\eta = 1$, which ties the unit of length (and time) to $m_{\text{scalar}}^{-1} = 1/\sqrt{2}$. The scalar core is resolved by at least three lattice points up to a center-of-mass speed of $v \approx 0.94$–0.96, which is indicated explicitly in the diagrams in Fig. 2. (It is higher in the $\beta = 4$ simulations because those have $a = 0.1$.) The initial string separation is fixed to $5\sqrt{2\beta}\gamma(v)m_{\text{scalar}}^{-1} = 5\sqrt{\beta}\gamma(v)$. This would be about 5 times the actual core radii for $\beta = 1$ but as β increases, the core sizes increase, and for large β one has to check that the gauge cores do not overlap in the initial configuration. For $\beta = 64$ the overlap in total energy from the tails of the gauge cores is less than 1% when $\gamma(v) = 1$, that is, when calculated on static vortices. Finally, the two-dimensional simulations of vortex-antivortex head-on collision and reemergence were done on an 800×800 grid with a lattice spacing of 0.1 and $\Delta t = 0.02$. In this way we resolve the vortex cores with at least 3 points up to a speed of $v \approx 0.985$. The initial separation is the same as in the 3D simulations. We used absorbing boundary conditions. In all simulations (2D and 3D), energy is conserved to better than 5% until the radiation hits the boundary (which determines the dynamical range).

IV. RESULTS

We simulated the collision of cosmic strings at $\beta = 1$, 3.9, 4.0, 4.1, 8, 16, 31, 32, 33, 49 and 64 for various speeds v and angles α to find the threshold velocity above which the strings effectively pass through each other. The results for selected values of β are shown in Fig. 2. Results for $\beta = 3.9$ and 4.1 were qualitatively similar to $\beta = 4$; also, results for $\beta = 31$, 32 and 33 were qualitatively similar. Some salient features have already been reported in Ref. [16].

The first thing that is apparent in Fig. 2 is that the minimum critical velocity for a second reconnection goes down as a function of β, in agreement with what was observed in [20]. The dependence of this lowest critical velocity $v_{c,\text{min}}$ with β and the range of collision angles for which it is observed is seen in Table I.

TABLE I. The lowest value of the critical velocity for double reconnection as a function of β, and the collision angles at which it is observed. The ranges in α indicate the possible existence of a plateau in the critical velocity.

β	$v_{c,\text{min}}$	α
4	0.92	42°
8	0.92	62°
16	0.90	90°–110°
32	0.88	80°–120°
49	0.88	85°–125°
64	0.86	105°–120°

Second, there is a new phenomenon of multiple intercommutations, which appears to be related to a change in the nature of the intermediate state from a nontopological blob of radiation to a loop.

The images of the intercommutation process in Figs. 3 and 4 show isosurfaces of the scalar field with $|\phi| = 0.4$. At this value, only about 20% of the potential energy is contained within them, but it allows us to visualize the evolution of the Higgs field most effectively. A tube twice the radius would contain about 60% of the energy. (To be precise, a threshold of $|\phi| = 0.8$, which has twice the thickness of the tubes shown, contains 62% of the scalar potential energy for $\beta = 16$, 57% for $\beta = 32$ and 52% for $\beta = 64$.)

It is clear from these images that the strings do not always intercommute once or twice, as previously observed, but also three and four times for particular values of the initial speed v and angle α. An odd number of reconnections results in overall intercommutation of the strings, and an even number in the strings effectively passing through, so we can still speak of a threshold velocity for the strings passing through. However, each reconnection creates small structure on the strings in the form of a left- and a right-moving kink. In some cases it is not easy to distinguish between one and three reconnections, or between two and four reconnections, just by looking at the energy isosurfaces in the intermediate state. But the resulting kinks are clearly visible in the final state and can be counted; in case of doubt, we use this criterion.

Successive reconnections therefore lead to left- or right-moving ''kink trains,'' groups of up to four closely spaced kinks (one for each intercommutation). The interkink distance within these trains is a few core widths, at the time of formation (see Fig. 3).

A multiple intercommutation process for type-II strings unfolds as follows. After the collision in which the strings exchange ends for the first time, two things can happen:

(a) For $\beta \geq 16$, an expanding loop forms after a short delay. If $v > v_c$, the loop catches up with the two receding strings, and these reconnect again through the loop. This creates a highly curved central region in each string. (Sometimes, for the lower collision angles, the loop is not as sharp as in Fig. 3 and the bridge is very pronounced, making the intermediate state look more like a junction.) The central regions will move toward each other and in some situations mediate a third reconnection (see Fig. 3). After the third reconnection, there are two almost antialigned string segments, and if they are receding sufficiently slowly a fourth reconnection is possible. This is the largest number of intercommutations we have seen, and only for $\beta = 16$. On the other hand, if $v < v_c$, the second reconnection does not take place because the string loop does not catch up with the strings. In this case it will contract again and eventually decay

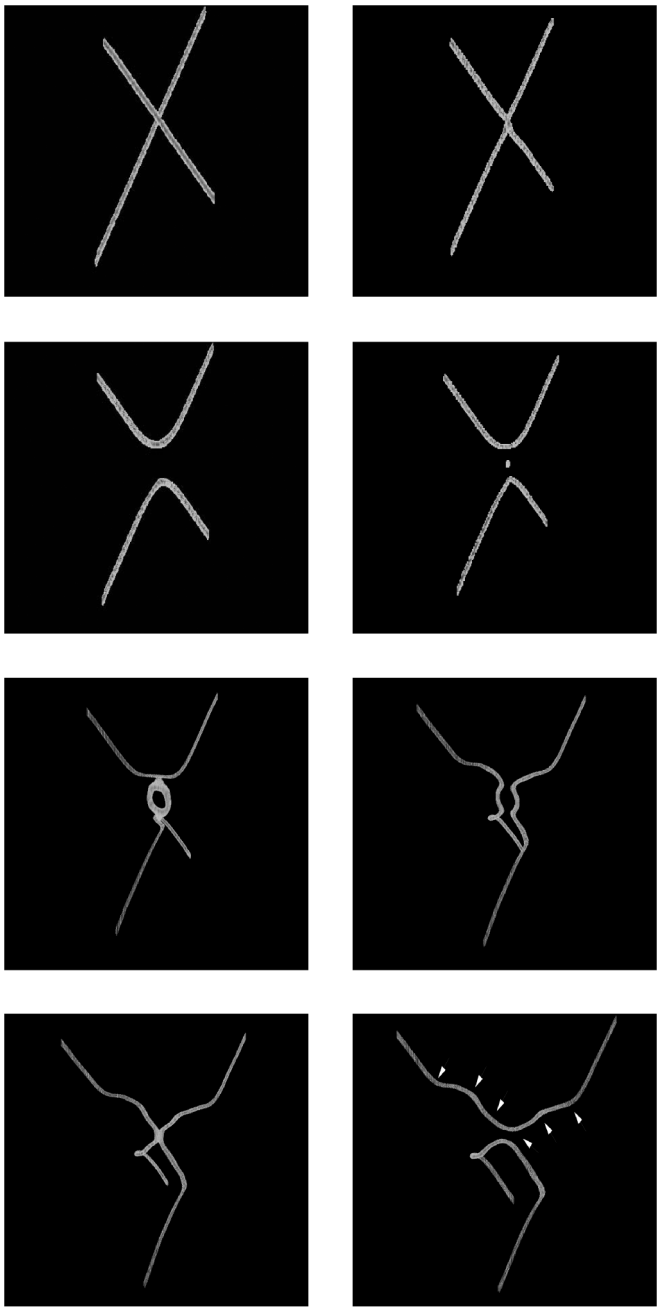

FIG. 3. Isosurfaces of the scalar field with $|\phi|/\eta \leq 0.4$ for a collision with ($\beta = 32$, $\alpha = 122.7$, $v = 0.88$) showing a triple intercommutation. From left to right, top to bottom: snapshots at $t = 3$, 4.7, 5, 6.9, 10, 17, 20, 22. Time is measured in inverse scalar masses (see text). At $t = 4.7$ (top right), the strings collide. Notice the distortion around the point of collision (see also Fig. 6). After the first intercommutation, a loop emerges at $t = 6.9$ (second row right). The loop catches up with the receding strings and intercommutes at the connection points ($t = 10$, second intercommutation, third row left), creating a highly curved central region in each string ($t = 17$, third row right). These move towards each other and produce a third intercommutation at $t = 20$ (fourth row left). Two sets of three closely spaced, left- and right-moving kinks (indicated by arrows on the upper string) are visible on each of the strings in the last panel.

into radiation, sometimes after one or a few oscillations.

Triple intercommutations are quite generic for collision speeds and angles on the boundary between the regions in parameter space where we observe one and two reconnections. For $\beta = 64$ we see a few triple intercommutations in a window around $v \sim 0.87$, $\alpha \sim 94°$. The box is already somewhat small, and we expect a larger box with increased dynamical range would show more multiple intercommutations, but this remains to be confirmed.

(b) For $1 < \beta \leq 8$ the energy isosurfaces look somewhat similar, but they reveal a very different intermediate state. The loop in Fig. 4 is just a blob of radiation with no topological features: the (covariant) phase of the Higgs field around the ''vortex'' that makes the loop shows no net winding around the loop, $\int_0^{2\pi}(\partial_\theta \mathrm{Arg}(\phi))d\theta = 0$. This is clearly visible in the third time step, where the loop meets the string bridges, breaks and is absorbed—a real loop of string would not be able to break if it carried a net winding. In this case the maximum number of

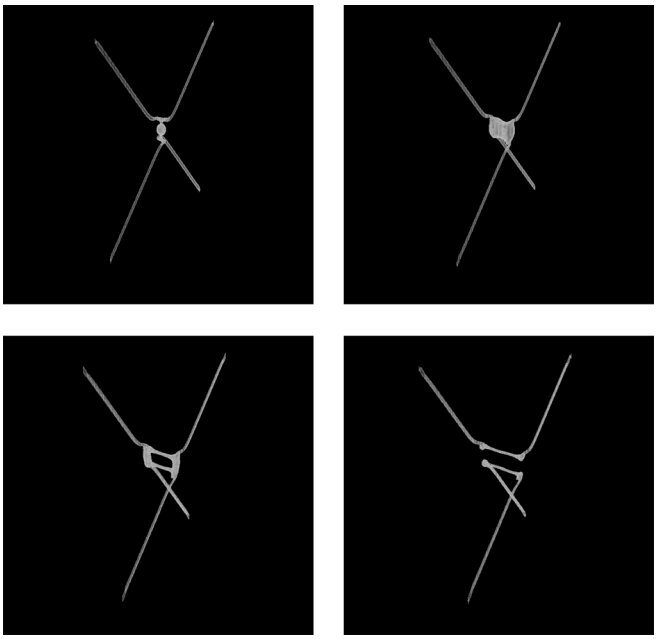

FIG. 4. After the first intercommutation, a radiation blob emerges. The blob catches up with the bridge and is absorbed. However, before it is absorbed, a loop seems to be formed (bottom right panel). This loop is not topological; it breaks resulting in ''Dracula's teeth.'' ($\beta = 4$, $\alpha = 122.7$, $v = 0.98$). The interaction between the blob and the strings slows them down, facilitating a second reconnection, but—unlike in Fig. 3—the blob by itself cannot mediate this second reconnection. From left to right,top to bottom: snapshots at $t = 2$, 4.5, 6.5, 8. Note the antialignment of the bridging segments between the strings, as in Fig. 1.

reconnections is two. The blob slows down the receding strings (thereby lowering the critical velocity) and facilitates the second reconnection. However, whether or not the second intercommutation takes place is still determined by the string bridge (see Fig. 1). We therefore see, as expected, a good agreement between the data and Eqs. (1) and (2) in Fig. 2 for $\beta = 4$ and 8.

We now turn to the simulations of the 2D head-on collision of a vortex and an antivortex at ultrarelativistic speeds. The parameters (β, v) of the simulations we performed are listed in Table II. While we confirm the general picture of Ref. [25], we have slightly different results for the state after the collision:

(a) For $\beta \leq 6.2$, the emerging vortex and antivortex settle in a bound, oscillating state, which completely decays into radiation for all speeds between $0.9 \leq v \leq 0.98$. This behavior extends to the $\beta < 4$ regime studied by Myers *et al.* [25], who interpreted the outcome as the reemergence, back-to-back, of the original pair. We see no evidence of this

TABLE II. The parameters (β, v) of the 2D simulations of vortex-antivortex collisions described in the text. The simulations in **boldface** are those where the vortex-antivortex pair reemerges as if they had passed through. In all other cases the pair annihilates into radiation, sometimes after forming a short-lived pulsating bound state. In the simulations in parentheses, the vortex-antivortex pair annihilate directly into radiation. The case $\beta = 4$, $v = 0.95$, indicated by an asterisk (*), is shown in Fig. 5.

β	v
1	0.8, 0.85, 0.9, 0.95
1.01	0.8, 0.85, 0.9, 0.95
2	0.9
3	0.9
4	(0.5), (0.6), (0.7), 0.8, 0.85, 0.9, 0.95*, 0.98
4.1	0.85, 0.9, 0.95, 0.98
4.2	0.9, 0.95, 0.98
4.3	0.9, 0.95, 0.98
4.4	0.9, 0.95, 0.98
4.5	0.9
4.6	0.9
4.7	0.9
4.8	0.9, 0.95, 0.98
4.9	0.9
5	0.9, 0.95, 0.98
6	0.9, 0.95, 0.98
6.2	0.85, 0.9, 0.95, 0.98
6.4	0.85, 0.9, 0.95, **0.98**
6.6	0.85, 0.9, 0.95, **0.98**
6.8	0.85, 0.9, 0.95, **0.98**
7	0.85, 0.9, **0.95**, **0.98**
8	0.85, 0.9, **0.95**, **0.98**
32	**0.7**, **0.8**, **0.85**, **0.875** **0.9**, **0.925**, **0.95**, **0.98**

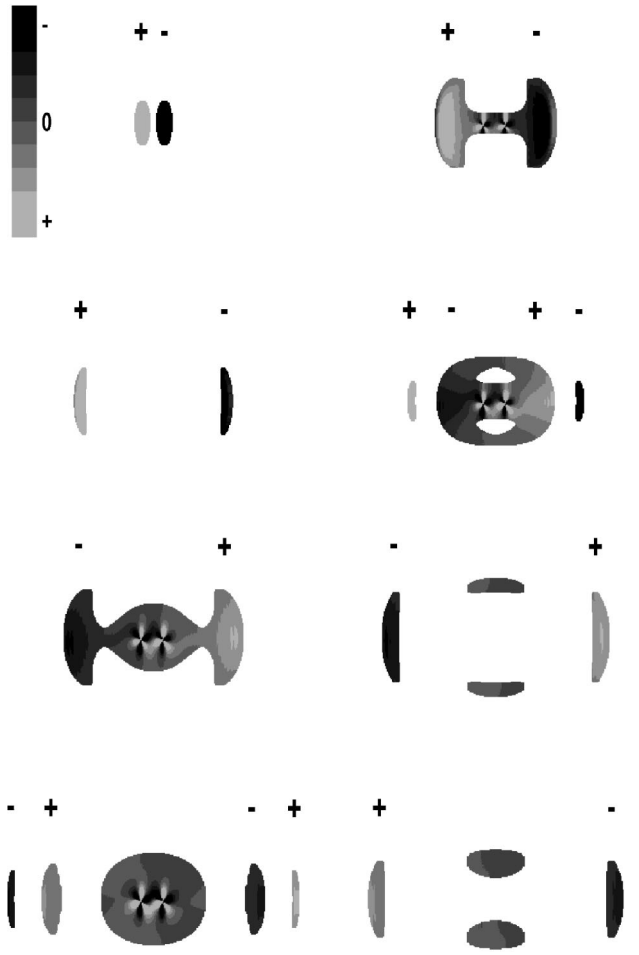

FIG. 5. A typical 2D head-on collision of a vortex and antivortex in the regime where the outcome is a radiating bound state (β below 6.2). The figure shows the magnetic field of a vortex and antivortex collision with $\beta = 4$ and $v = 0.95$. All other parameters and time scales are as in the previous 3D simulations. Only points with $|\phi|/\eta \leq 0.9$ are shown. Black to intermediate grey indicates the magnetic field pointing into the page $(-)$, while intermediate to light grey indicates the magnetic field pointing out of the page $(+)$. Black (light grey) indicate points whose magnetic field is $\geq 20\%$ of the maximum magnetic-field value, which is attained at the core of the incoming vortex (antivortex). The intermediate shades of grey are in decreasing steps of 5% (seen in the first panel). From left to right and top to bottom: The panels show snapshots at $t = 0$, 7, 9, 10, 12, 14, 17 and 18. First, we see the vortex and antivortex at $t = 0$. Second, we see a ''pair'' reform ($t = 7$), but they are actually two blobs of radiation. In the third figure ($t = 9$), we see a configuration which could be mistaken for a back-to-back reemergence. However, we then see a second blob forming ($t = 10$), and the first pair fizzling out. The magnetic field oscillates around zero. At $t = 12$ the second pair (blob) forms and some radiation is exchanged. By this time, the magnetic field of the first pair has already switched sign. This proves that the first pair had no topology. In the sixth panel ($t = 14$), polarity is opposite to that in the second panel, but there is also radiation in the perpendicular direction. At $t = 17$ a third blob forms and decays into radiation ($t = 18$). This process continues for the dynamical range of the simulation or until all energy is radiated away.

reemergence. A typical configuration after the collision is shown in Fig. 5. Although some time steps could be mistaken for back-to-back reemergence of the vortex-antivortex pair, subsequent evolution makes it clear it is only localized radiation.

Note also that, since the vortex-antivortex pair never reforms after the collision, the expectation of back-to-back reemergence, suggested in [42] by analogy with the global vortex case, also does not apply.

(b) For $\beta \geq 6.4$ and high collision speeds, the pair reemerges as if they passed through, and the critical velocity above which the vortex-antivortex pair passes through each other goes down with increasing β, from around $v = 0.98$ for $\beta = 6.4$ to (β, v): (6.6, 0.98), (6.8, 0.98), (7, 0.95), (8, 0.95) and (32, $<$0.7). This agrees with Ref. [25].

V. DISCUSSION

Our results suggest some interesting differences between the $\beta \gg 1$ regime and the much more studied $\beta = 1$ regime when it comes to the intercommutation behavior and the resulting small scale structure. Some of these differences can be traced back to the core interactions, in particular, the repulsion between parallel, deep type-II strings, which in a 3D setting can distort the impact angles and velocities of the strings. The angular distortions can be parametrized and could in principle be incorporated into numerical simulations of cosmic string networks and analytic studies of small scale structure.

A. Multiple reconnections and the nature of the intermediate state

As reported in [16], we have observed a qualitative change in the process determining the second intercommutation. For $1 \leq \beta \leq 8$ we see the emergence of a blob of radiation after the first intercommutation. A blob cannot cause a second intercommutation by itself; it is absorbed when it reaches the strings. In this case, whether or not the second intercommutation takes place is determined by the geometry after the first intercommutation. This situation is well described by Eqs. (1) and (2), as found in [20]. On the other hand, for $\beta \geq 16$ we see the emergence of an expanding topological loop that mediates the second intercommutation. We compare this transition with the reemergence of the vortex-antivortex pair in highly relativistic two-dimensional collisions: as β increases, the critical speed for 2D vortex-antivortex reemergence goes down *below* the critical speed for double reconnection in 3D (and even below the 3D universal bound on the critical speed $v \sim 0.77$ [16]; see the next subsection). Therefore, for sufficiently large β, reemergence of the vortex-antivortex pair is unavoidable. In 3D the re-emergent vortex-antivortex pair leads to a loop. Thus, for $\beta \geq 16$, the outcome is always the same: the loop always forms. However, whether or not this loop leads to a second reconnection depends on whether the loop catches up with the receding strings, which is, in turn, determined by the velocity and angle of the strings before the collision: for high v there is a second reconnection, for lower v there is only one reconnection. It is also in this loop-mediated regime, of which the lower bound is between $\beta = 8$ and $\beta = 16$ according to our simulations, where the multiple or higher order intercommutations take place. By contrast, for low β, the critical speed in 2D for the reemergence of the vortex-antivortex pair is so high that we do not see the emergence of a string loop in 3D. Instead, we see what we describe as a radiation blob, the 3D equivalent of the bound, oscillating state in 2D. An interesting open question is to identify more precisely the value of β (between 8 and 16) at which the transition between these two regimes occurs in 3D.

B. The critical velocity for double reconnection: β dependence, angular dependence and a universal lower bound

The dependence of v_c with the collision angle shows that, as we go deeper into the type-II regime, core interactions are playing an important role, especially at high collision angles. With better resolution and more data points than in [20] we actually see a difference with the $\beta \approx 1$ behavior. The best fits with Eqs. (1) and (2) do not quite agree with the data for large β (e.g. $\beta > 16$). These fits underestimate the critical velocity for impact angles close to antiparallel (or else do not properly account for impact angles below 90°). Discarding data points with impact angles larger than 150° leads to the fits shown in Fig. 2 with the dotted line. We found for $\beta = 4$, 8 following parameters: $w_t = 0.202$, 0.238 and $\delta_t = 136.4°$, 139.3°. For $\beta = 16$, 32, 49 and 64 we found $w_t = 0.328$, 0.357, 0.261, 0.408, $\delta_t = 144.0°$, 136.1°, 139.0°, 135.7°, respectively. (We note that for $\beta = 49$ the fit has fewer relevant data points.)

The deviation between the fits and the data at high collision angle is, by itself, not so surprising since in the deep type-II regime two things change: First, the appearance of the loop means the angle between the string segments is not expected to be relevant. The second intercommutation will occur if the loop touches the receding segments, irrespective of their mutual angle. Second, the core interaction affects the state before the collision; it produces a torque that deforms the strings and tends to antialign the colliding segments. This means the true collision angle is actually larger than the initial value. The torque results from the attraction between vortex and antivortex and vortex-vortex repulsion in the orthogonal plane, which compete in the type-I regime but add up in type-II.

One might expect that a modification of the Nambu-Goto fit of [20] to account for this offset in collision angle should give a better fit in the deep type-II regime:

$$w = \sin[(\alpha - \alpha_0)/2]\frac{1}{\gamma(v)}, \quad (4)$$

$$\cos(\delta/2) = \frac{\cos[(\alpha - \alpha_0)/2]/(v\gamma(v))}{\sqrt{1 + (\cos[(\alpha - \alpha_0)/2]/(v\gamma(v)))^2}}, \quad (5)$$

with α_0 negative. This expectation is not borne out by the data. In fact, if anything, the data prefer a modification with a *smaller* angle (positive α_0—see Table III). And this can be understood by looking at Fig. 6. Although the actual collision angle (the angle at the point of collision) is larger than α, the motion of the strings after the collision is determined by an *effective* collision angle ξ that is *smaller* than α. This is because the antialignment causes a larger portion of string to be annihilated so, after a quick transient, the strings look as if they had collided with angle $\xi < \alpha$ and the bridge segments (see Fig. 1) are further apart than they would have been in the absence of a torque.

If the collision is sufficiently close to antiparallel, the relation between the angle of approach, α, and the effective collision angle ξ is universal (see Fig. 6): $\tan\alpha/2 = (1 + \sin\xi/2)/\cos\xi/2$, that is, $\xi = 2\alpha - \pi$, or $\alpha_0 = \pi - \alpha$, expected to be valid for large α. This one-parameter fit is shown with a dashed line in Fig. 2. The fit parameter is $w_{\rm crit}$ and it has values (β, $w_{\rm crit}$): (16, 0.233), (32, 0.243), (49, 0.251) and (64, 0.275).

The offset in collision angle (see Table III) for $\beta \geq 16$ indicates that the torque is strong even at very high collision speeds and suggests strong distortions for low speed collisions. This is potentially very interesting from the point of view of the radiation coming from cosmic strings. Usually, the radiation bursts from reconnection are subdominant to those from cusps and kinks [43,44]. But here reconnection bursts are enhanced because longer segments of string are annihilated. The amount of radiation produced by cosmic string reconnection might therefore be somewhat larger in deep type-II collisions than would be expected from analytic, Nambu-Goto arguments.

Finally, our results appear to confirm the claim [20] that the critical speed goes down with increasing β, from $v_c \sim 0.96$ at $\beta = 1$ to $v_c \sim 0.86$ at $\beta = 64$, although this reduction cannot go on indefinitely. A crude (universal) lower bound for v_c follows from energy conservation [16]: if the strings antialign locally and a portion L of each string is annihilated, the maximum energy available to the loop is $2L\gamma = 2\pi R$, with R the maximum loop radius. If $R < L/2$, the second intercommutation cannot take place, which happens for $v < \sqrt{1 - 4/\pi^2} \sim 0.77$. These values of v_c are to be contrasted with the average root mean square velocity of the network, which has not yet been investigated for type-II strings. (Known values range from $v_{rms} = 1/\sqrt{2} \sim 0.71$ for Nambu-Goto strings in flat space to $0.63 - 0.51$ in field theory simulations with $\beta = 1$ with cosmic expansion [45,46].) So, double intercommutations may be less rare than in type-I collisions, but they are still rare events.

TABLE III. The best fit parameters of Eqs. (4) and (5). A positive (negative) offset α_0 indicates the actual collision angle is smaller (larger) than in the initial configuration. We see that α_0 becomes positive for $\beta \geq 16$ and remains positive and relatively large.

β	w_t	δ_t	α_0
4	0.227	137.2	−20.7
8	0.249	141.5	−6.8
16	0.238	223.9	50.6
32	0.282	229.7	32.8
49	0.266	233.3	48.1
64	0.257	234.7	58.7

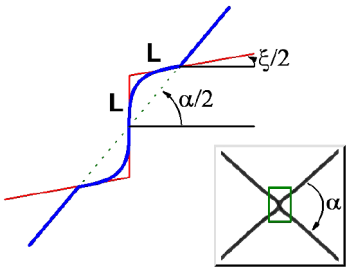

FIG. 6 (color online). The bending of the strings at the point of collision due to the intervortex potential, modeled in the figure as a sinusoidal perturbation. α is the initial collision angle when the strings are approaching but still far apart. The torque tends to antialign the segments around the collision point. (See the top right panel of Fig. 3.) Subsequently, a vertical segment of length $\sim 2L$ will annihilate from each string, leaving the receding strings as if they had collided with angle ξ. Note that, although the torque tends to increase the collision angle, the effective reconnection angle ξ is actually *smaller* than the initial collision angle α.

VI. SUMMARY AND OUTLOOK

We have investigated numerically the intercommutation of Abelian Higgs strings in the deep type-II regime for selected values of $\beta \equiv m^2_{\rm scalar}/m^2_{\rm gauge} \gg 1$ up to $\beta = 64$, the highest value studied to date. Our study shows interesting differences with the $\beta = 1$ behavior and raises some puzzling questions. New effects arise due to the strong interactions of the string cores. Multiple reconnections were already reported in [16], and also a qualitative change in the intermediate state after the first reconnection, with truly topological loops appearing only for $\beta \geq 16$. It is also in this regime ($\beta \geq 16$) where we find the higher order (three or more) intercommutations. Further work is needed to understand if the window closes for $\beta > 64$. We see fewer multiple intercommutations, but this could be simply due to the limitations of the dynamical range.

As β increases, we find a lower critical velocity for double (or multiple) reconnections, in agreement with

[20], but for very large β we are unable to describe the angular dependence in detail. The fit derived in [20] works well for $\beta \leq 8$ and maybe even for $\beta = 16$ but not in the deep type-II regime $\beta \geq 32$. The interaction between the magnetic cores produces a torque that tends to antialign the string segments, so the actual collision angle is higher than in the initial configuration, but this is true only around the collision point, and this portion of string quickly disappears. In fact, due to this antialignment, the collision results in the annihilation of a larger segment of string, so in fact the strings behave as if they that had collided with a *smaller* angle. The simplest way to model the bending of the string, as a sinusoidal excitation, is shown in Fig. 6 and gives the angle ξ in terms of α: $\xi/2 = \alpha - \pi/2$. Using $\xi/2$ instead of $\alpha/2$ in Eq. (1), we find a one-parameter fit to our data with initial collision angles higher than 120°. The fit is shown with a dashed line in Fig. 2.

Even for lower collision angles, the fit derived in [20], with or without an adjustment to include the torque between the colliding strings, does not fully describe the angle dependence of the critical velocity. Our data (see Fig. 2) is possibly better described in the deep type-II regime by a curve of opposite concavity with a plateau between collision angles of 80° and 120°. A more detailed study is necessary to understand the angle dependence of the critical velocity.

We also simulated two-dimensional vortex-antivortex head-on collisions in an attempt to understand the new 3D effects. We confirmed the result of Myers *et al.* [25] that for high enough collision speed the vortex-antivortex pair reemerges some time after the collision. The critical speed for reemergence goes down with increasing β, and for $\beta = 32$ is already lower than $v \sim 0.7$. On the other hand, for $\beta < 8$ the velocity needed for the vortex-antivortex pair to reemerge is so high ($v \geq 0.98$) that we see only a (bound) radiating state. In particular, for $\beta \leq 4$ Myers *et al.* report the backscatter of the vortex-antivortex pair whereas we always see a radiating bound state. This is however not inconsistent with [25] given their much smaller dynamical range (see Fig. 5). So we see a transition between reemergence in forward direction vs a bound radiating state; we never see backscatter.

Further work is needed to determine the critical β, in 2D head-on vortex-antivortex collisions, that distinguishes the regime where a bound radiating state forms from the regime where the vortex-antivortex pair reemerge as if they had passed through. We can locate this transition somewhere around $6.2 \leq \beta \leq 6.4$, but the main problem in determining this critical β is the high collision speed ($v > 0.98$) needed for reemergence, which leads to very bad resolution.

Our expectation is that the 2D radiating bound states at low β should roughly correspond to the 3D blob, and that 2D forward reemergence should correspond to the 3D loop. For not too large β (in particular below 6.2), the critical velocity for passing through in 2D is so high ($> 0.98c$) that we do not probe it in either the 2D or 3D simulations; we always see a radiation blob. As β increases, the critical velocity for passing through in 2D goes down, and at high β (in particular ≥ 32) the critical velocity for forward reemergence is so low ($< 0.7c$) that all the 3D simulations are in this regime, and all show loop formation.

Although suggestive, our interpretation of the results is not conclusive. To confirm this picture one should study the transition region $8 \leq \beta \leq 32$, $0.7 \leq v \leq 0.95$ both in 2D and 3D and verify the extent of this correlation. (It is important to note that we have no data between $\beta = 8$ and $\beta = 16$.) Also, we do not necessarily expect a precise, one-to-one correspondence in the critical values of β and v because the energy requirements to reform a vortex-antivortex pair in 2D are different from those needed to form a loop in 3D.

The effect on the cosmological signatures of strings is hard to predict, as the stronger core interactions in the deep type-II regime affect energy loss mechanisms in several, competing, ways [16]. In general, we expect a relative enhancement of the radiation contribution from kinks and reconnections at the expense of cusps (suppressed by the kinks [47,48]) and loops (suppressed by the lower critical velocity for double reconnection).

Regarding kinks, a new feature is the presence of kink trains resulting from multiple reconnections. These are rare, but once a kink train is formed, its decay time is comparable to that of a single kink, and because of its microscopic size (only a few core widths in length), it is very unlikely to be disrupted by intercommutation with another string segment. We conclude that the small scale structure of strongly type-II Abelian Higgs string networks could be somewhat more clustered than the predictions based on the Nambu-Goto approximation with $P = 1$ [49–51], although nowhere near the proliferation of kinks expected in a network with junctions [52].

Regarding reconnections, they are enhanced in two ways. First, while we confirm that strongly type-II ANO strings *always reconnect* ($P = 1$), an *effective* intercommutation probability $P_{\text{eff}} \leq 1$ due to multiple reconnections will still lead to denser networks and therefore more reconnections. Second, most of these will be at low velocity, and we have argued that antialignment plays a role even in relativistic speed collisions, so we expect a strong effect in low velocity collisions. So we would expect stronger and more frequent bursts of radiation and cosmic rays than for other string types (lower β and also superstrings) where reconnection bursts are always negligible or subdominant [43,44].

Further work is needed to understand these effects quantitatively, and how they affect the cosmological bounds. But the upshot of the work presented here is that core interactions are expected to cause significant differences with respect to the predictions from both Nambu-Goto

strings and field theory Abelian Higgs strings in the Bogomol'nyi limit.

Finally, our results confirm once again that Abelian Higgs strings *always reconnect*, even at ultrarelativistic speeds ($P = 1$); unlike for other types of defects [25,35], and against naïve expectations, the only way in which strings can pass through each other appears to be by an even number of reconnections.

ACKNOWLEDGMENTS

We are grateful to Roland de Putter, Mark Jackson, Paul Shellard and Jon Urrestilla for discussions. This work was supported by the Netherlands Organization for Scientific Research (NWO) under the VICI programme. We acknowledge partial support by the Consolider-ingenio programme No. CDS2007-00042.

[1] T. W. B. Kibble, J. Phys. A **9**, 1387 (1976).
[2] A. Vilenkin and E. Shellard, *Cosmic Strings and Other Topological Defects* (Cambridge University Press, Cambridge, England, 1994).
[3] M. B. Hindmarsh and T. W. B. Kibble, Rep. Prog. Phys. **58**, 477 (1995).
[4] J. Polchinski in Lectures at the Cargèse Summer School (2004) (unpublished) [arXiv:hep-th/0412244].
[5] A.-C. Davis and T. Kibble, Contemp. Phys. **46**, 313 (2005).
[6] E. J. Copeland and T. W. B. Kibble, Proc. R. Soc. A **466**, 623 (2010).
[7] M. Sakellariadou, Nucl. Phys. B, Proc. Suppl. **192–193**, 68 (2009).
[8] A. Achúcarro and C. J. A. P. Martins in *Encyclopedia of Complexity and Systems Science*, edited by Robert Meyers (Springer, New York, 2009), Vol. 3, pp. 1641–1660.
[9] C. Ringeval, Adv. Astron. **2010**, 1 (2010).
[10] E. J. Copeland, L. Pogosian, and T. Vachaspati, Classical Quantum Gravity **28**, 204009 (2011).
[11] M. Hindmarsh, arXiv:1106.0391.
[12] R. Jeannerot, Phys. Rev. D **56**, 6205 (1997).
[13] R. Jeannerot, J. Rocher, and M. Sakellariadou, Phys. Rev. D **68**, 103514 (2003).
[14] M. Majumdar and A. Christine-Davis, J. High Energy Phys. 03 (2002) 056.
[15] S. Sarangi and S. H. H. Tye, Phys. Lett. B **536**, 185 (2002).
[16] A. Achúcarro and G. Verbiest, Phys. Rev. Lett. **105**, 021601 (2010).
[17] L. Jacobs and C. Rebbi, Phys. Rev. B **19**, 4486 (1979).
[18] E. Shellard, Nucl. Phys. **B283**, 624 (1987).
[19] R. Matzner, Comput. Phys. **2**, 51 (1988).
[20] A. Achúcarro and R. de Putter, Phys. Rev. D **74**, 121701 (R) (2006).
[21] A. A. Abrikosov, Sov. Phys. JETP **5**, 1174 (1957).
[22] H. B. Nielsen and P. Olesen, Nucl. Phys. **B61**, 45 (1973).
[23] M. G. Jackson, N. T. Jones, and J. Polchinski, J. High Energy Phys. 10 (2005) 013.
[24] A. Avgoustidis and E. P. S. Shellard, Phys. Rev. D **73**, 041301 (2006).
[25] E. Myers, C. Rebbi, and R. Strilka, Phys. Rev. D **45**, 1355 (1992).
[26] K. J. M. Moriarty, E. Myers, and C. Rebbi, J. Comput. Phys. **88**, 467 (1990).
[27] L. M. A. Bettencourt and T. W. B. Kibble, Phys. Lett. B **332**, 297 (1994).
[28] L. M. Bettencourt, P. Laguna, and R. A. Matzner, Phys. Rev. Lett. **78**, 2066 (1997).
[29] E. J. Copeland, T. W. B. Kibble, and D. A. Steer, Phys. Rev. D **75**, 065024 (2007).
[30] E. J. Copeland, T. W. B. Kibble, and D. A. Steer, Phys. Rev. Lett. **97**, 021602 (2006).
[31] P. Salmi, A. Achúcarro, E. Copeland, T. Kibble, R. de Putter, and D. Steer, Phys. Rev. D **77**, 041701 (2008).
[32] J. Polchinski, Phys. Lett. B **209**, 252 (1988).
[33] K. Hashimoto and D. Tong, J. Cosmol. Astropart. Phys. 09 (2005) 004.
[34] E. J. Copeland and N. Turok, Report No. FERMILAB-PUB-86-127-A, 1986.
[35] J. Giblin, T. John, L. Hui, E. A. Lim, and I.-S. Yang, Phys. Rev. D **82**, 045019 (2010).
[36] N. S. Manton, Phys. Lett. **110B**, 54 (1982).
[37] E. Bogomol'nyi, Sov. J. Nucl. Phys. **24**, 449 (1976).
[38] P. J. Ruback, Nucl. Phys. **B296**, 669 (1988).
[39] T. M. Samols, Commun. Math. Phys. **145**, 149 (1992).
[40] A. Hanany and K. Hashimoto, J. High Energy Phys. 06 (2005) 021.
[41] M. Eto, K. Hashimoto, G. Marmorini, M. Nitta, K. Ohashi *et al.*, Phys. Rev. Lett. **98**, 091602 (2007).
[42] C. Rosenzweig and A. M. Srivastava, Phys. Rev. D **43**, 4029 (1991).
[43] T. Damour and A. Vilenkin, Phys. Rev. D **64**, 064008 (2001).
[44] M. G. Jackson and X. Siemens, J. High Energy Phys. 06 (2009) 089.
[45] J. N. Moore, E. P. S. Shellard, and C. J. A. P. Martins, Phys. Rev. D **65**, 023503 (2001).
[46] M. Hindmarsh, S. Stuckey, and N. Bevis, Phys. Rev. D **79**, 123504 (2009).
[47] T. Kibble and N. Turok, Phys. Lett. **116B**, 141 (1982).
[48] D. Garfinkle and T. Vachaspati, Phys. Rev. D **36**, 2229 (1987).
[49] T. W. B. Kibble and E. J. Copeland, Phys. Scr. **T36**, 153 (1991).
[50] J. Polchinski and J. V. Rocha, Phys. Rev. D **74**, 083504 (2006).
[51] E. J. Copeland and T. W. B. Kibble, Phys. Rev. D **80**, 123523 (2009).
[52] P. Binetruy, A. Bohe, T. Hertog, and D. A. Steer, Phys. Rev. D **82**, 083524 (2010).